

To be submitted to the *Astrophysical Journal Supp.*

## New theoretical line list for the $B' \ ^2\Sigma^+ \leftarrow X \ ^2\Sigma^+$ system of $^{24}\text{MgH}$

S. Skory<sup>1</sup>, P. F. Weck & P. C. Stancil

*Department of Physics and Astronomy and Center for Simulation Physics,  
The University of Georgia, Athens, GA 30602-2451*

weck@physast.uga.edu, stancil@physast.uga.edu

K. Kirby

*Harvard-Smithsonian Center for Astrophysics  
60 Garden St., Cambridge, MA 02138*

kkirby@cfa.harvard.edu

### ABSTRACT

Fully quantum-mechanical techniques have been applied to compute the complete line list for the  $B' \ ^2\Sigma^+ \leftarrow X \ ^2\Sigma^+$  system of  $^{24}\text{MgH}$ . The list includes transition energies and oscillator strengths over the wavelength range 11,850-32,130  $\text{cm}^{-1}$ , for all possible allowed transitions from the ground electronic state vibrational levels  $v'' = 0 - 11$ . This list was computed using the best available *ab initio* potential energies and dipole transition moment function, with the former adjusted to account for experimental data. The agreement of the current calculations with previous theoretical results and the line list of Kurucz is discussed. Although spectroscopic accuracy for a particular line cannot be claimed for our calculations, comparison is made with the recent astronomical measurements of Wallace et al. A line list for pure rovibrational transitions in the  $X \ ^2\Sigma^+$  state is also presented.

*Subject headings:* molecular data — stars: atmospheres — stars: late-type

---

<sup>1</sup>Summer 2001 NSF-REU Program Fellow at the University of Georgia. Current address: Department of Physics, University of California, Berkeley, CA 94720-7300, sskory@uclink4.berkeley.edu

## 1. Introduction

Magnesium hydride is an important molecule in various astrophysical environments. The electronic bands of MgH have been detected over a wide range of stellar atmospheres such as the solar photosphere (Sotirovski 1972; Grevesse & Sauval 1973), sunspot umbrae (Wallace et al. 1999), F-K giants in the Milky Way halo and halos of other Local Group galaxies (Majewski et al. 2000), and nearby L-dwarfs (Reid et al. 2000). Spectroscopic lines of MgH are used as a probe of surface gravity in late-type stars (Bonnell & Bell 1993), as well as to determine the magnesium isotope abundances (Wallace et al. 1999; Gay & Lambert 2000).

The strong  $A \ ^2\Pi - X \ ^2\Sigma^+$  band system of MgH in the visible region of the spectrum has been extensively studied in the laboratory for many decades both in absorption and emission (Balfour 1970a,b; Balfour & Cartwright 1976; Bernath, Black & Brault 1985, and references therein). The  $B' \ ^2\Sigma^+ - X \ ^2\Sigma^+$  system, discovered experimentally in emission over the wavelength range 21,500-26,000  $\text{cm}^{-1}$  by Balfour & Cartwright (1975, 1976) and explored further to  $\sim 12,000 \text{ cm}^{-1}$  by Balfour & Lindgren (1978), has never been detected in absorption in the laboratory to our knowledge. In response to the suggestion by Balfour & Cartwright (1975) of the importance of the dissociation mechanism for this electronic transition, the theoretical study of Kirby, Saxon & Liu (1979) demonstrated that, within the Franck-Condon approximation, only 24% of the  $B' \leftarrow X$  oscillator strength from the  $v'' = 0$  vibrational level of the  $X$  state goes into dissociating the molecule. The weakness of the  $B' \leftarrow X$  system is due to the dipole transition moment function crossing through zero in the vicinity of the equilibrium internuclear separation of the  $X \ ^2\Sigma^+$  state.

Because the lines are so weak, identification and measurement of the frequencies of the MgH  $B' \leftarrow X$  absorption lines in astronomical sources have been performed only recently. Wallace et al. (1998) reported in sunspot umbral spectra three series of lines between 13,173 and 13,580  $\text{cm}^{-1}$  which were identified afterwards as the  $R$  and  $P$  branches of the 0-7 band and the  $P$  branch of the 1-8 band of the  $B' \leftarrow X$  transition of  $^{24}\text{MgH}$ . Beyond this wavelength region, bounded by the strong 0-1 head of the TiO  $\gamma$  bands (Ram et al. 1999) and by the  $\Delta v = -1$  series of the CaH  $A - X$  bands (Weck, Stancil & Kirby 2003b), Wallace et al. (1999) extended the identification to the lines of the 0-3, 0-4, 0-5, 0-6, 0-7, 1-3, 1-4, 1-7 and 1-8 bands of the  $B' \leftarrow X$  system of  $^{24}\text{MgH}$ .

While astronomical and laboratory measurements of spectral lines remain the most accurate spectroscopic reference, complete line lists and energy level data are essential to reproducing the global opacity needed for any reliable calculation of structure or radiation transport in stellar atmospheres (Hauschildt & Baron 1999). For the  $B' \leftarrow X$  system of MgH, the only complete theoretical line list is found in the extensive compilations of Kurucz

(1993a). However, in these compilations a number of approximations have been made which at times lead to significant loss of accuracy.

In this work, we apply fully quantum-mechanical techniques to compute the complete line list for the  $B' \leftarrow X$  transition of  $^{24}\text{MgH}$ . The parameters of the calculation are adjusted to force agreement with laboratory measurements, although we cannot claim spectroscopic accuracy for a particular line. Details of this optimization procedure are given in section 2, along with an overview of the theory of molecular rotational lines. In section 3, we present our results of energy level and line list calculations for the  $B' \leftarrow X$  and the  $X \leftarrow X$  transitions and compare them to the theoretical calculations of Kirby et al. (1979). The agreement of our data with the recent astronomical measurements of Wallace et al. (1999) and with the previous line list of Kurucz (1993a) is also discussed.

## 2. Molecular theory

### 2.1. Potential energy curves and dipole transition moments

The *ab initio* potential energy curves calculated by Saxon, Kirby & Liu (1978) have been used in this work for the  $B' \ ^2\Sigma^+$  and  $X \ ^2\Sigma^+$  electronic states of MgH. Their configuration interaction wave function includes singly- to triply-excited configurations (SDTCI) in a large Slater-type basis set, calculated at internuclear separations  $R = 2.2$  to  $9.5 \ a_0$ . The derived spectroscopic constants agree well with experimental data.

In order to optimize our calculations, the dissociation energy,  $D_0^0$ , was adjusted to coincide with the experimental value  $10,243.26 \text{ cm}^{-1}$  for the  $X \ ^2\Sigma^+$  state (Balfour & Lindgren 1978), and  $10,046.89 \text{ cm}^{-1}$  for the  $B' \ ^2\Sigma^+$  state of  $^{24}\text{MgH}$ . The  $D_0^0(B' \ ^2\Sigma^+)$  was evaluated from the experimental electronic dissociation energy,  $D_e$ , and spectroscopic constants given in Saxon et al. (1978) using the relation

$$D_0^0 = D_e - \frac{\omega_e}{2} + \frac{\omega_e x_e}{4} - \frac{\omega_e y_e}{8}. \quad (1)$$

Consequently, shifts in energy<sup>2</sup> of  $+8.740 \times 10^{-4} \text{ a.u.}$  and  $-1.8358 \times 10^{-3} \text{ a.u.}$  have been applied, respectively, to the  $X \ ^2\Sigma^+$  and  $B' \ ^2\Sigma^+$  potential energy curves calculated by Saxon et al. (1978) over the entire internuclear distance range.

The relative energies between the two potential curves were further shifted to match the energy difference corresponding to the pure (0,0) vibronic transition. The value of

---

<sup>2</sup>Atomic units are used throughout this section unless otherwise stated.

$T_e = 2.779$  eV ( $22,410$  cm $^{-1}$ ) determined experimentally by Balfour & Cartwright (1976) was adopted in our calculations.

Beyond the range of internuclear separations,  $R = 2.2$  a $_0$  to  $9.5$  a $_0$ , considered by Saxon et al. (1978), the potential energy curves have been extrapolated in two different ways. For internuclear distances  $R > 9.5$  a $_0$ , a smooth fit to the *ab initio* potentials has been performed using the long-range dispersion expansion

$$V(R) = -\frac{C_6}{R^6} - \frac{C_8}{R^8} - \frac{C_{10}}{R^{10}}, \quad (2)$$

where  $C_6$ ,  $C_8$  and  $C_{10}$  are the usual van der Waals coefficients corresponding to the dipole-dipole, dipole-quadrupole, and the sum of quadrupole-quadrupole and dipole-octupole interactions, respectively. For the  $X$   $^2\Sigma^+$  ground state, we used  $C_6^X = 57.8$  calculated by A. Derevianko (2001, private communication). The values of  $C_8^X = 2,490$  and  $C_{10}^X = 115,000$ , calculated by Standard & Certain (1985), were also used in this work.

To our knowledge, no data have been reported for the van der Waals coefficients of the  $B'$   $^2\Sigma^+$  state of MgH. Therefore, theoretical estimates have been obtained using a technique based on the London formula (CRC Handbook of Chemistry & Physics 1988),

$$C_6 = \frac{3 \alpha_H \Delta E_H \times \alpha_{Mg} \Delta E_{Mg}}{2 \Delta E_H + \Delta E_{Mg}}, \quad (3)$$

where  $\alpha_H = 4.5$  a.u. and  $\Delta E_H = 0.375$  a.u. are the exact values, respectively, of the static dipole polarizability and the  $1s \rightarrow 2p$  transition energy of H. Since the  $X$   $^2\Sigma^+$  and  $B'$   $^2\Sigma^+$  states dissociate to Mg( $3s^2$   $^1S$ )+H( $1s$   $^2S$ ) and Mg( $3s3p$   $^3P^0$ )+H( $1s$   $^2S$ ), respectively, the experimental  $\Delta E_{Mg}(3s^2$   $^1S \rightarrow 3s3p$   $^1P^0)$  and  $\Delta E_{Mg}(3s3p$   $^3P^0 \rightarrow 3s3p$   $^3D)$  tabulated in Mérawa et al. (2001) have been used to calculate estimates for  $C_6^X$  and  $C_6^{B'}$ . The values of  $\alpha_{Mg}(3$   $^1S) = 71.2$  a.u. and  $\alpha_{Mg}(3$   $^3P) = 87.0$  a.u. calculated by Mérawa et al. (2001) in the mixed gauge form were adopted. The ratio  $C_6^{B'}/C_6^X$  of these estimates was used further as a scaling factor for the  $C_n^X$  calculated by Derevianko (2001) and Standard & Certain (1985) in order to obtain final  $C_n^{B'}$  values, resulting in  $C_6^{B'} = 56.9$ ,  $C_8^{B'} = 2,451$  and  $C_{10}^{B'} = 113,205$ . The accuracy of this procedure is unknown, but given that the static dipole polarizabilities and the dominant transition energies of the ground and excited Mg have similar values, the  $C_6$  values are expected to be comparable.

For internuclear distances  $R < 2.2$  a $_0$ , the potential curves of both the  $X$   $^2\Sigma^+$  and the  $B'$   $^2\Sigma^+$  electronic states have been fitted to the short-range interaction exponential form  $A \exp(-BR) + C$ .

In a similar way, the dipole transition moment for  $B'$   $^2\Sigma^+ \leftarrow X$   $^2\Sigma^+$  and the dipole moment of the  $X$  state calculated by Saxon et al. (1978) have been used over the range

$R = 2.2 a_0$  to  $9.5 a_0$ , and extrapolated by an exponential fit for both the short- and long-range interactions. The dipole moment function of  $X$  was smoothly forced to zero both at the united-atom and the separated-atom limits. At  $R = 0$ , the dipole transition moment was constrained to 1.5 a.u., the value of aluminum (NIST Atomic Spectra Database 1999), and was extrapolated to zero at large internuclear separations.

## 2.2. Line and band oscillator strengths

For a discrete absorption transition to a given bound rovibrational state  $v'N'$  of the final electronic state from a rovibrational state  $v''N''$  of the initial electronic state, the line oscillator strength can be expressed by (Larsson 1983)

$$f_{v'N',v''N''}^{ab} = \frac{2}{3} \Delta E_{v'N',v''N''} \frac{S_{N'}(N'')}{2N'' + 1}, \quad (4)$$

where  $\Delta E_{v'N',v''N''}$  is the absorbed photon energy, in hartrees, and  $S_{N'}(N'')$  is the line strength for a molecular transition,

$$S_{N'}(N'') = | \langle \chi_{v'N'} | D(R) | \chi_{v''N''} \rangle |^2 S_{N'}(N''), \quad (5)$$

as defined by Whiting & Nicholls (1974). Here,  $D(R)$ , in atomic units of  $ea_0$ , is the electric dipole transition moment responsible for transitions between the initial and final electronic states, and the dimensionless Hönl-London factors,  $S_{N'}(N'')$ , can be expressed for a  $\Sigma \leftarrow \Sigma$  electronic transition as

$$S_{N'}(N'') = \begin{cases} N'', & N' = N'' - 1 \text{ (P-branch)} \\ N'' + 1, & N' = N'' + 1 \text{ (R-branch)}. \end{cases} \quad (6)$$

The rovibrational wave functions  $\chi_{vN}(R)$  of Eq. (5) are solutions of the radial nuclear Schrödinger equation,

$$\left[ -\frac{1}{2\mu} \frac{d^2}{dR^2} + E_{el}(R) + \frac{N(N+1)}{2\mu R^2} - E_{vN} \right] \chi_{vN}(R) = 0, \quad (7)$$

where  $\mu$  is the reduced mass of the system,  $N$  is the rotational quantum number corresponding to the angular momentum of nuclear rotation neglecting the nuclear and electronic spins and  $E_{el}(R)$  and  $E_{vN}$  are the electronic potential energy and rovibrational energy eigenvalues, respectively.

For the sake of comparison with the band oscillator strengths  $f_{v'v''}^{ab}$  calculated by Kirby

et al. (1979), we used the following relation<sup>3</sup> between band and line oscillator strengths, as defined in Eq. (4),

$$\begin{aligned} f_{v'v''}^{ab} &= \frac{g_{N',N''}^{ab}}{S_{N'}(N'')} f_{v'N',v''N''}^{ab} \\ &= \frac{(2 - \delta_{0,\Lambda''+\Lambda'}) (2N'' + 1)}{(2 - \delta_{0,\Lambda''}) S_{N'}(N'')} f_{v'N',v''N''}^{ab}, \end{aligned} \quad (8)$$

with  $N'' = 0$  and  $N' = 1$  and where  $g_{N',N''}^{ab}$ , equal to  $(2N'' + 1)$  for a  $\Sigma \leftarrow \Sigma$  electronic transition, is a degeneracy factor arising from spin-splitting in both final and initial electronic states, an effect which is neglected in this work.

### 3. Results and discussion

The energy levels,  $E_{vN}$ , and the rovibrational wave functions,  $\chi_{vJ}(R)$ , of Eq. (7) have been calculated by solving the radial nuclear Schrödinger equation for the final and initial electronic states by standard Numerov techniques (Cooley 1961). Calculations have been performed on a grid with stepsize  $1 \times 10^{-3} a_0$  for the integration, over a range of internuclear distances from  $R = 0.5 a_0$  to  $200 a_0$ . This outer limit value of the integration range was chosen intentionally large in order to obtain all the roots of the radial equation as the dissociation limit is reached. The reduced mass adopted for  $^{24}\text{MgH}$  was  $0.9671852 \text{ u}^4 = 1763.064 \text{ a.u.}$  (Huber & Herzberg 1979).

The vibrational binding energies and the corresponding  $\Delta G(v + 1/2) = G(v + 1) - G(v)$  of the  $X \ ^2\Sigma^+$  and  $B' \ ^2\Sigma^+$  states obtained in the present study are given in Table 1, along with the previous theoretical values of Saxon et al. (1978) and the measurements of Balfour & Cartwright (1976). Our results are found to be in excellent agreement with the  $\Delta G$ 's calculated by Saxon et al. (1978), with differences less than  $1 \text{ cm}^{-1}$  up to  $v'' = 7$  and  $v' = 10$  for the  $X \ ^2\Sigma^+$  and  $B' \ ^2\Sigma^+$  states, respectively. For the  $X$  state, the largest discrepancy with experimental data is of the order of  $\sim 20 \text{ cm}^{-1}$ , thus improving on the previous calculations which showed a maximum disagreement of  $\sim 35 \text{ cm}^{-1}$  for  $v'' = 8$ . For the  $B'$  state, comparison to experimental data reveals that the Saxon et al. (1978) potential is somewhat broader than in reality since the calculated  $\Delta G$ 's are found to systematically underestimate experimental values by up to  $17 \text{ cm}^{-1}$  for  $v' = 8$ . In addition, our long-range

---

<sup>3</sup>The first equality of Eq. (8) corrects a misprint in Eq. (4) of Weck et al. (2003a) where  $g_{N',N''}^{ab}$  should appear in the numerator.

<sup>4</sup>In atomic mass units, Aston's scale

fitting procedure to the interaction potential yields 1 and 4 additional vibrational levels near the dissociation threshold for the  $X$  and  $B'$  states, respectively, such that  $v''_{\max} = 11$  and  $v'_{\max} = 20$ . The maximum  $N$  for each  $v$  is also indicated in Table 1, giving a total of 301 rovibrational levels for the  $X$  state and 815 for the  $B'$  state.

In Table 2, vibrational oscillator strengths are reported for the  $\Delta v = 1, 2,$  and  $3$  transitions within the  $X \ ^2\Sigma^+$  state. These are calculated using equations (4) and (5), with  $D(R)$  the  $X$ -state dipole moment, and both  $v'N'$  and  $v''N''$  levels originating in the ground electronic state. Only those oscillator strengths which have dipole matrix elements larger than  $1 \times 10^{-3} e a_0$  are given. Our results are in excellent overall agreement with the previous calculations of Kirby et al. (1979), as could be expected from the close agreement of the  $X$  state vibrational energy levels for both sets of calculations. The small differences can be mainly attributed to our fitting procedure to incorporate accurate experimental data. The maximum values of the vibrational oscillator strength correspond to the  $v' = 4 \leftarrow v'' = 3$  transition, and the  $3 \leftarrow 2$  and  $5 \leftarrow 4$  transitions which bracket the  $4 \leftarrow 3$ . This can be straightforwardly explained by the presence of an extremum in the  $X$  dipole moment function at  $4.4 a_0$  (Saxon et al. 1978), which coincides with the outer turning point location of the  $v'' = 4$  vibrational level. The complete distribution of line oscillator strengths for rovibrational transitions in the  $X \ ^2\Sigma^+$  state are shown in Figure 1, including the pure rotational transitions which appear for transition energies less than  $390 \text{ cm}^{-1}$ .

The band oscillator strengths and transitions energies for the  $B' \ ^2\Sigma^+ \leftarrow X \ ^2\Sigma^+$  system are given in Table 3 for the transitions between the vibrational states  $v'' = 0 - 3$  and  $v' = 0 - 14$ . The current calculations satisfactorily reproduce the theoretical results of Kirby et al. (1979). The 0-0 band is very weak and the oscillator strength distribution is dominated by off-diagonal transitions with large  $\Delta v$ . The weakness of the transitions from the low-lying  $v''$  vibrational states is due to the dipole transition moment function crossing through zero in the vicinity of the equilibrium internuclear distance of the  $X \ ^2\Sigma^+$  state and to the shift of the  $B'$  equilibrium distance by  $\sim 1.6 a_0$  longward of the  $X$  value.

Theoretical line oscillator strengths and transition energies for the 0-7, 1-8, 0-3, 0-4, 0-5, 0-6, 0-7, 1-3, 1-4, 1-7 and 1-8 bands of the  $B' \leftarrow X$  system of  $^{24}\text{MgH}$  are given in Table 4 along with the observed lines in the sunspot spectrum identified by Wallace et al. (1999). The largest discrepancies with available data appear for the strong 1-8 band, with transition energy differences ranging between  $35.4 \text{ cm}^{-1}$  [ $P(5)$  line] and  $53.6 \text{ cm}^{-1}$  [ $R(14)$  line]. In general, because the potential energy curves are the most uncertain for high-lying vibrational and rotational energy levels, transitions involving high  $v, N$  levels show the largest discrepancies with respect to experimental transition energies. We note that the agreement of our calculations with observations is optimal for transitions between low-lying

rovibrational states, as a consequence of our procedure to force agreement with laboratory measurements.

Line oscillator strengths<sup>5</sup> are shown in Figure 2 for the  $B' \ ^2\Sigma^+ \leftarrow X \ ^2\Sigma^+$  transition as a function of the energy of the absorbed photon. The series of peaks with intensities larger by a factor of two than all other lines in the same wavelength region correspond to the  $N' = 1 \leftarrow N'' = 0$  lines of the  $R$  branch. The strongest  $R(0)$  transitions occur for atypically large vibrational transitions, with  $\Delta v = v'' - v' = 7$  for the three most intense lines of the oscillator strength distribution at  $13,580 \text{ cm}^{-1}$  (0-7 band),  $13,611 \text{ cm}^{-1}$  (1-8 band) and  $13,721 \text{ cm}^{-1}$  (2-9 band). As the photon energy increases, the  $\Delta v$  values for these  $R(0)$  lines tend to decrease, as can be seen in the peak series with successively the  $R(0)$  lines of the 0-6, 0-5, 1-5, 1-4, 2-4, 2-3 and 3-3 bands. As noted in the discussion of Table 3, the weakness of the lines from low lying  $v''$  states is due to the presence of a zero in the  $B' - X$  dipole transition moment function near the equilibrium distance of the  $X \ ^2\Sigma^+$  state. Moreover, this function shows an extremum at  $5.0 a_0$ , the equilibrium distance of the  $B' \ ^2\Sigma^+$  state. This has the effect of enhancing the intensity of transitions to low-lying  $v'$  states from high-lying  $v''$  states, since the outer turning point of the latter tends to approach  $5.0 a_0$ . This is clearly illustrated by the strong  $R(0)$  lines of the 1-8, 0-7 and 2-9 bands for which the overlap of the initial and final wave functions with the extremum of the transition dipole moment is optimal.

The product  $g_{J',J''} \cdot f_{v',v'',J',J''}$ , the so-called  $gf$ -value, is plotted in Figure 3 as a function of the absorbed photon energy where comparison is made to the line list of Kurucz (1993a). As is shown, our  $gf$ -values agree well with the previous calculations which were obtained with a model rotational Hamiltonian using spectroscopic constants (Kurucz 1993b). The qualitative discrepancies existing between both sets of calculations may be mainly attributed to the loss of accuracy of model Hamiltonian approaches as the quantum numbers  $v$  and/or  $N$  increase.

#### 4. Conclusion

A comprehensive and complete theoretical line list for the  $B' \ ^2\Sigma^+ \leftarrow X \ ^2\Sigma^+$  transition of  $^{24}\text{MgH}$  was constructed, using a combination of theoretical and experimental data on the potential energies and dipole transition moment. Our calculations are in excellent agreement with previous theoretical studies and show strong lines for atypically large vibrational transitions, thus reflecting the particular character of the  $B' \leftarrow X$  dipole transition moment

---

<sup>5</sup>The complete list of MgH oscillator strength data is available online at the UGA Molecular Opacity Project database website <http://www.physast.uga.edu/ugamop/>

function. Comparison with the recent astronomical measurements of Wallace et al. (1999) reveals that, although our line list reproduces observations with reasonable agreement, the transition energies are not of spectroscopic accuracy. Nevertheless, these new  $B' \leftarrow X$  and  $X \leftarrow X$  line data described in this work should significantly improve synthetic spectrum calculations. This has been shown recently in Weck et al. (2003a) for effective temperatures pertaining to L and M type stars, where differences in the opacity arise when comparing the resulting spectra to calculations using the previous data of Kurucz (1993a).

This work was supported by NASA grant NAG5-10551, and partially by NSF through the REU Program at the University of Georgia and a grant for the Institute for Theoretical Atomic, Molecular and Optical Physics at Harvard University and Smithsonian Astrophysical Observatory. Some of the calculations were performed on the IBM SP2 and the SGI Origin of the UGA EITS.

## REFERENCES

- Balfour, W. J. 1970a, *J. Phys. B.*, 3, 1749
- Balfour, W. J. 1970b, *ApJ*, 162, 1031
- Balfour, W. J., & Cartwright, H. M. 1975, *Chem. Phys. Lett.*, 32, 82
- Balfour, W. J., & Cartwright, H. M. 1976, *A&AS*, 26, 389
- Balfour, W. J., & Lindgren, B. 1978, *Can. J. Phys.*, 56, 767
- Bernath, P. F., Black, J. H., & Brault, J. W. 1985, *ApJ*, 298, 375
- Bonnell, J. T. & Bell, R. A. 1993, *MNRAS*, 264, 334
- Condon, U., & Shortley, G.H. 1935, *The Theory of Atomic Spectra*, (London: Cambridge Univ. Press)
- Cooley, J. W. 1961, *Math. Computation*, 15, 363
- CRC Handbook of Chemistry & Physics 1988, 69th ed. (Boca Raton: CRC Press)
- Gay, P. L. & Lambert, D. L. 2000, *ApJ*, 533, 260
- Grevesse, N., & Sauval, A. J. 1973, *Astr. Ap.*, 27, 29
- Hauschildt, P. H., & Baron, E. 1999, *J. Comput. Appl. Math.*, 102, 41

- Huber, K. P. & Herzberg, G. 1979, *Molecular Spectra and Molecular Structure*, Vol. IV, Constants of Diatomic Molecules (New York: Van Nostrand Reinhold)
- Kirby, K., Saxon, R. P., & Liu, B. 1979, *ApJ*, 231, 637
- Kurucz, R. L. 1993a, CD-ROM No.15 Diatomic molecular data for opacity calculations (Harvard-Smithsonian Center for Astrophysics)
- Kurucz, R. L. 1993b, *Molecules in the Stellar Environment*, ed. U. G. Jørgensen (Berlin: Springer-Verlag), p. 282
- Larsson, M. 1983, *A&A*, 128, 291
- Majewski, S. R., Ostheimer, J. C., Kunkel, W. E., & Patterson, R. J. 2000, *AJ*, 120, 2550
- Mérava, M., Bégué, D., Rérat, M., & Pouchan, C. 2001, *Chem. Phys. Lett.*, 334, 403-410
- NIST Atomic Spectra Database 1999, [http://aeldata.phy.nist.gov/cgi-bin/AtData/main\\_asd](http://aeldata.phy.nist.gov/cgi-bin/AtData/main_asd)
- Ram, R. S., Bernath, P. F., Dulick, M., & Wallace, L. 1999, *ApJS*, 122, 331
- Reid, I. N., Kirkpatrick, J. D., Gizis, J. E., Dahn, C. C., Monet, D. G., Williams, R. J., Liebert, J., & Burgasser, A. J. 2000, *AJ*, 119, 369
- Saxon, R. P., Kirby, K., & Liu, B. 1978, *J. Chem. Phys.*, 12, 5301
- Sotirovski, S. 1972, *A&AS*, 6, 85
- Standard, J. M., & Certain, P. R. 1985, *J. Chem. Phys.*, 83, 3002
- Wallace, L., Livingston, W.C., Bernath, P. F., & Ram, R. S. 1998, *An Atlas of the Sunspot Umbral Spectrum in the Red and Infrared from 8900 to 15050 cm<sup>-1</sup>* (Tech. Rep. 98-002; Tucson: NSO)
- Wallace, L., Hinkle, K., Li, G., & Bernath, P. F. 1999, *ApJ*, 524, 454
- Weck, P. F., Schweitzer, A., Stancil, P. C., Hauschildt, P. H., & Kirby, K. 2003a, *ApJ*, 582, 1059
- Weck, P. F., Stancil, P. C., & Kirby, K. 2003b, *J. Chem. Phys.*, in press
- Whiting, E. E., & Nicholls, R. W. 1974, *ApJS*, 27, 1

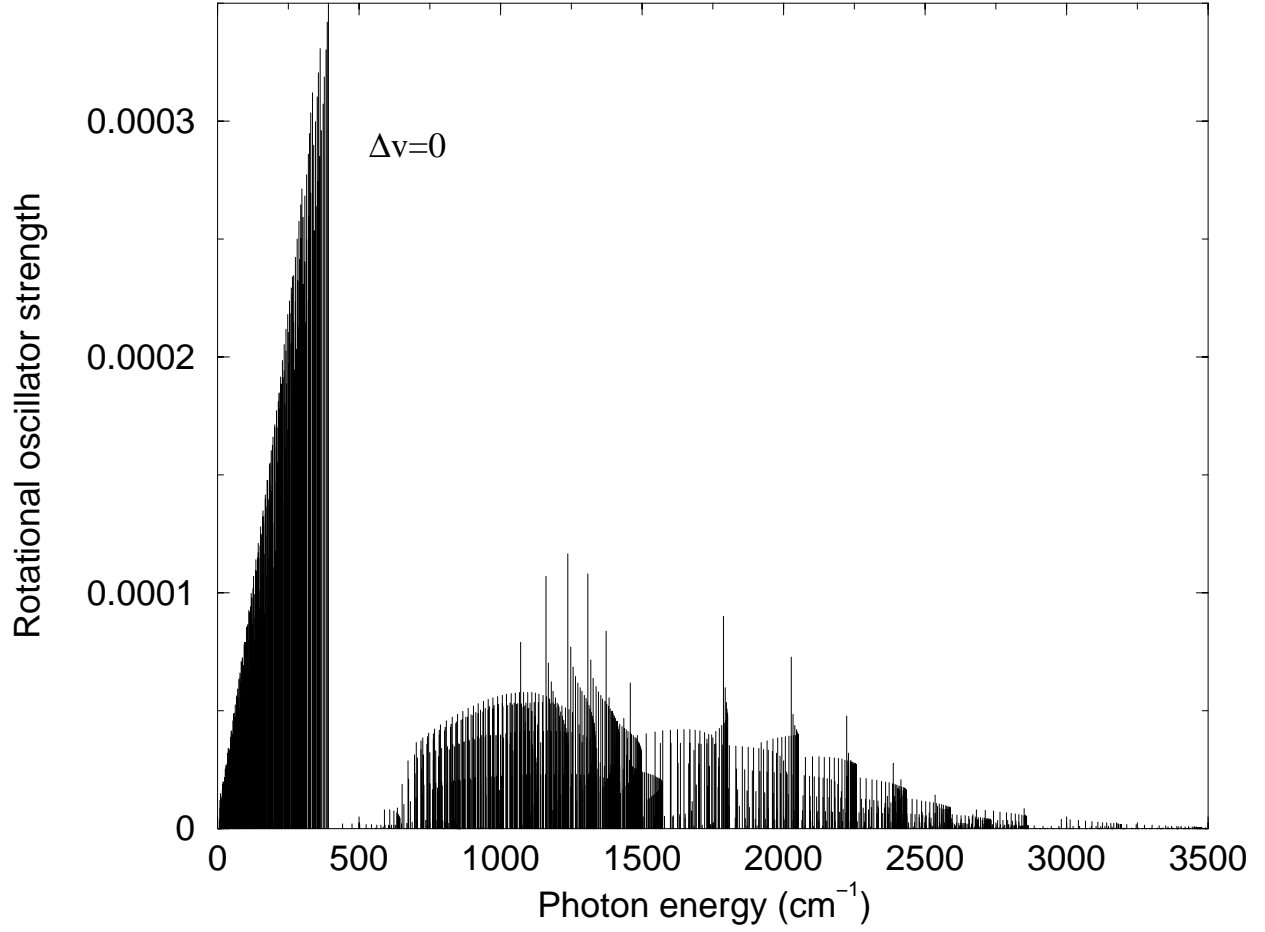


Fig. 1.— Line oscillator strengths  $f_{v'N',v''N''}$  for the rovibrational transitions in the  $X^2\Sigma^+$  state as a function of the absorbed photon energy.

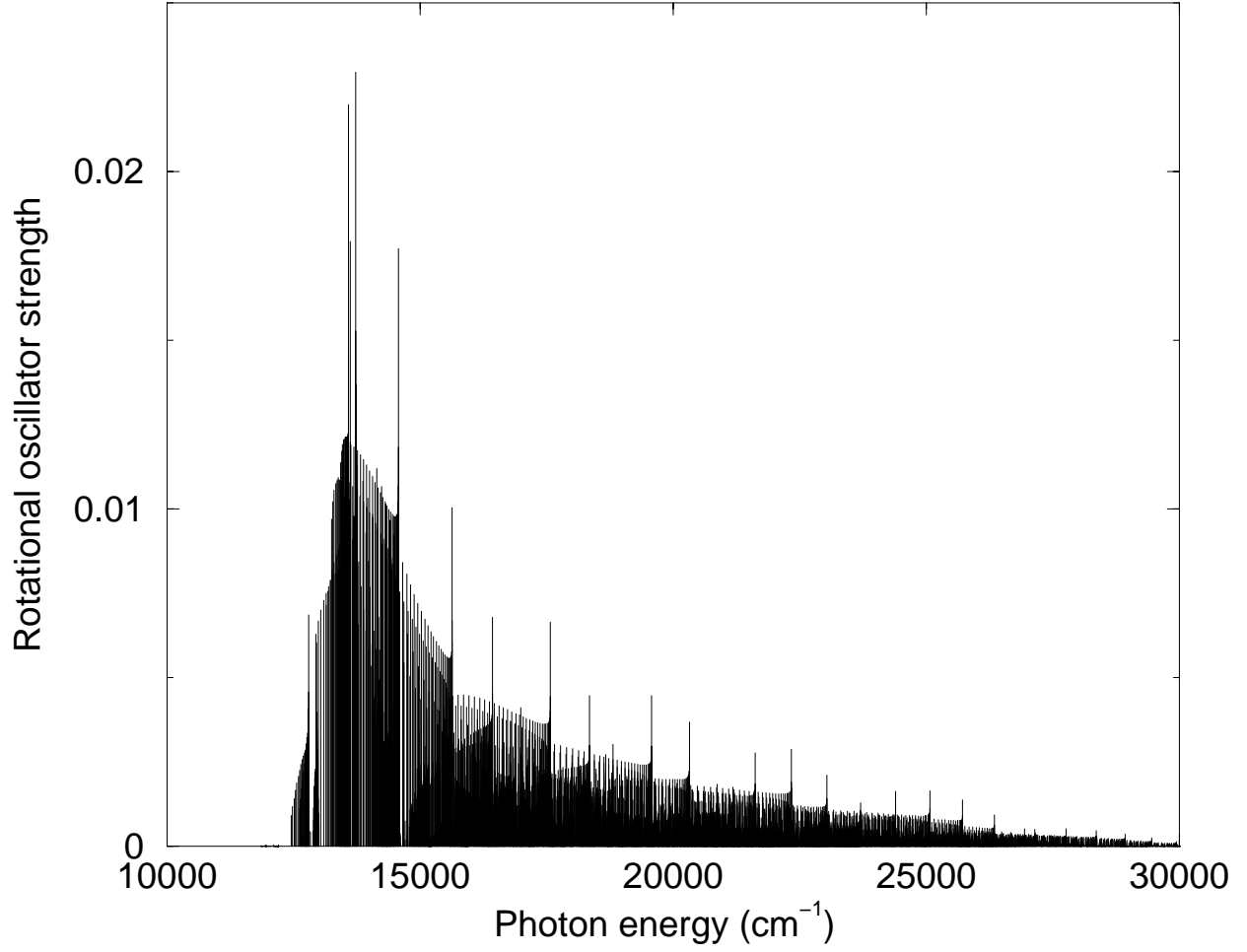


Fig. 2.— Line oscillator strengths  $f_{v'N',v''N''}$  for the  $B' \ ^2\Sigma^+ \leftarrow X \ ^2\Sigma^+$  system as a function of the absorbed photon energy.

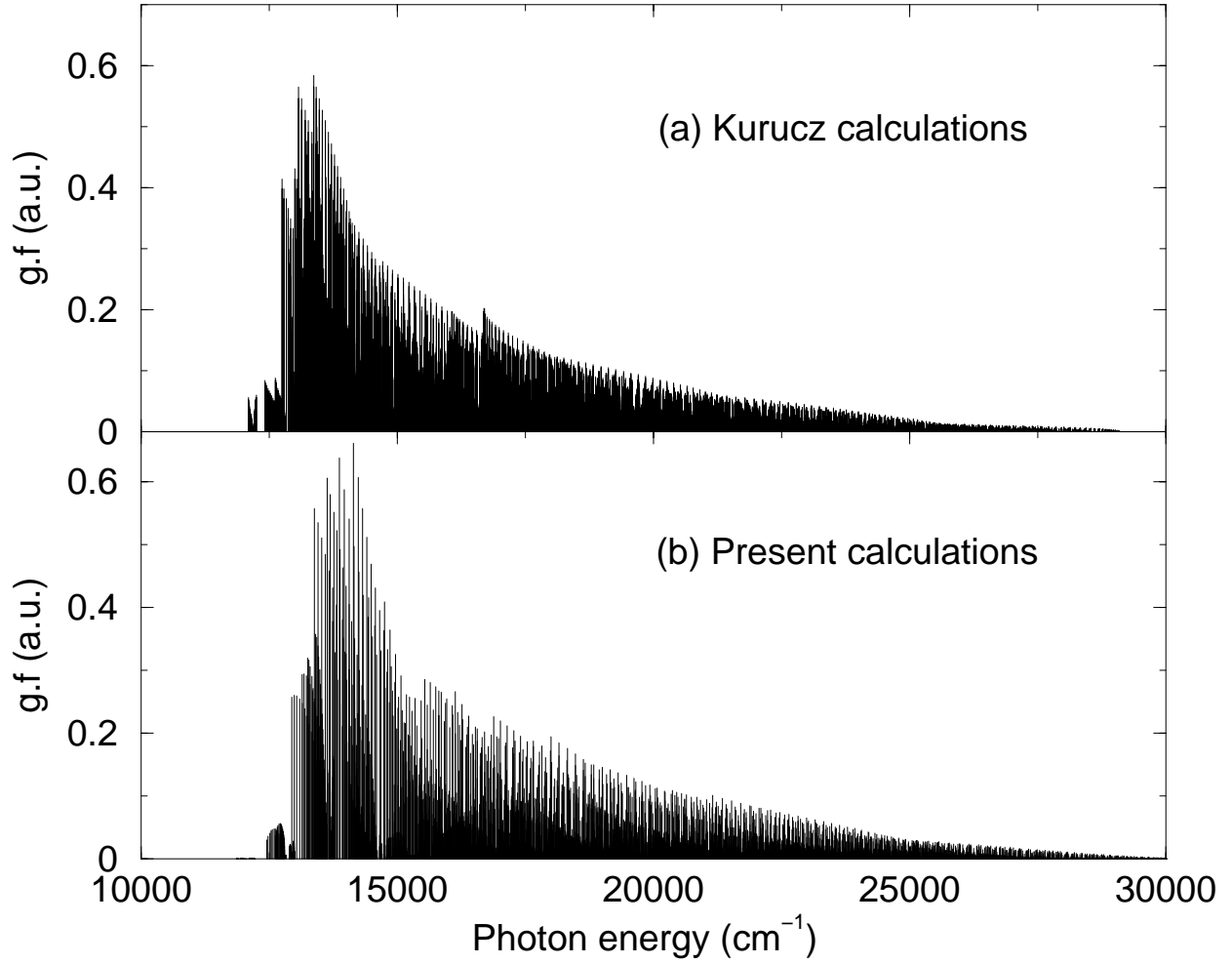


Fig. 3.— Values of  $g_{N',N''} \cdot f_{v'N',v''N''}$  as a function of the absorbed photon energy for the  $B' \ ^2\Sigma^+ \leftarrow X \ ^2\Sigma^+$  system. (a) Calculations of Kurucz (1993a). (b) Present calculations.

Table 1. Vibrational Binding Energies<sup>a</sup> and  $\Delta G(v + 1/2)$  in  $\text{cm}^{-1}$  for the  $X \ ^2\Sigma^+$  and  $B' \ ^2\Sigma^+$  States

State	$v$	$N_{max}^b$	B. E. <sup>b</sup>	$\Delta G(v + 1/2)$		
				Theory <sup>b</sup>	Saxon <sup>c</sup>	Expt. <sup>d</sup>
$X \ ^2\Sigma^+$	0	44	10243.2	1423.0	1423.0	1432.0
	1	41	8820.3	1361.4	1361.8	1368.7
	2	39	7458.9	1297.0	1297.2	1301.5
	3	35	6161.9	1227.6	1227.5	1229.1
	4	32	4934.2	1150.3	1150.3	1229.1
	5	29	3783.9	1061.7	1061.9	1055.3
	6	25	2722.2	956.3	956.3	941.3
	7	20	1765.9	822.6	822.7	799.0
	8	16	943.4	629.4	644.0	609.1
	9	10	314.0	220.9	391.5	...
	10	7	93.0	81.9	...	...
$B' \ ^2\Sigma^+$	11	3	11.4	...	...	...
	0	67	10046.9	792.1	792.7	805.2
	1	64	9254.8	769.2	769.0	780.4
	2	62	8485.6	745.6	745.3	760.0
	3	59	7740.0	721.3	721.7	735.8
	4	57	7018.7	697.6	697.9	712.2
	5	54	6321.1	674.2	674.3	688.8
	6	51	5646.9	649.8	649.7	664.2
	7	49	4997.1	623.6	623.3	638.8
	8	46	4373.5	594.7	594.6	610.9
	9	43	3778.8	562.3	562.6	...
	10	40	3216.5	526.2	525.9	...
	11	38	2690.3	487.1	482.8	...
	12	35	2203.2	445.2	432.1	...
	13	32	1758.0	399.7	378.1	...
	14	29	1358.3	352.2	339.1	...
	15	25	1006.1	305.6	317.5	...
16	22	700.5	264.4	...	...	

Table 1—Continued

State	$v$	$N_{max}^b$	B. E. <sup>b</sup>	$\Delta G(v + 1/2)$		
				Theory <sup>b</sup>	Saxon <sup>c</sup>	Expt. <sup>d</sup>
	17	18	436.1	220.1	...	...
	18	14	216.0	146.9	...	...
	19	8	69.1	67.6	...	...
	20	2	1.5	...	...	...

<sup>a</sup>Binding energies are given for rotationless vibrational levels.

<sup>b</sup>This work.

<sup>c</sup>Saxon et al. (1978).

<sup>d</sup>Balfour & Cartwright (1976).

Table 2. Vibrational Transition Oscillator Strengths\* within the  $X^2\Sigma^+$  State

$v' \setminus v''$	0	1	2	3	4	5
1.....	4.68(-5)	...	...	...	...	...
	4.76(-5)	...	...	...	...	...
	(1432.0)	...	...	...	...	...
2.....	1.72(-6)	8.38(-5)	...	...	...	...
	1.76(-6)	8.48(-5)	...	...	...	...
	(2800.7)	(1368.7)	...	...	...	...
3.....	1.1(-8)	6.05(-6)	1.08(-4)	...	...	...
	1.3(-8)	5.44(-6)	1.09(-4)	...	...	...
	(4102.2)	(2670.2)	(1301.5)	...	...	...
4.....	...	6.3(-8)	1.42(-5)	1.17(-4)	...	...
	...	5.1(-8)	1.41(-5)	1.18(-4)	...	...
	...	(3899.3)	(2530.6)	(1229.1)	...	...
5.....	...	...	2.4(-7)	2.78(-5)	1.07(-4)	...
	...	...	1.9(-7)	2.79(-5)	1.06(-4)	...
	...	...	(3678.7)	(2377.2)	(1148.1)	...
6.....	...	...	...	8.2(-7)	4.79(-5)	7.91(-5)
	...	...	...	6.8(-7)	4.89(-5)	7.81(-5)
	...	...	...	(3432.5)	(2203.4)	(1055.3)
7.....	...	...	...	...	2.69(-6)	7.27(-5)
	...	...	...	...	2.61(-6)	7.16(-5)
	...	...	...	...	(3144.7)	(1996.6)
8.....	...	...	...	...	7.0(-8)	8.49(-6)
	...	...	...	...	2.0(-8)	9.16(-6)
	...	...	...	...	(3943.7)	(2795.6)
9.....	...	...	...	...	...	5.3(-7)
	...	...	...	...	...	5.4(-7)
	...	...	...	...	...	(3404.7)

\*Vibrational transition oscillator strengths are given in a.u. and are calculated for rotational quantum numbers  $N'' = 0$  and  $N' = 1$ . Our results are listed on the first line, with the previous calculations of Kirby et al. (1979) on the second line, and with the transition energies in  $\text{cm}^{-1}$  given by Balfour & Lindgren (1978) below.

Table 3. Band Oscillator Strengths\* and Transition Energies† for the  $B' \ ^2\Sigma^+ \leftarrow X \ ^2\Sigma^+$  Band System

$v'$ ( $B' \ ^2\Sigma^+$ )	$(X^2\Sigma^+) \ v'' = 0$		$v'' = 1$		$v'' = 2$		$v'' = 3$	
	$E_{v'0}$	$f_{v'0}$	$E_{v'1}$	$f_{v'1}$	$E_{v'2}$	$f_{v'2}$	$E_{v'3}$	$f_{v'3}$
0.....	22087	7.16(-7)	20664	1.56(-5)	19303	1.55(-4)	18006	9.34(-4)
	22082	7.44(-7)	20651	1.58(-5)	19282	1.51(-4)	17980	9.30(-4)
1.....	22880	6.42(-6)	21456	1.09(-4)	20095	7.72(-4)	18798	3.03(-3)
	22887	6.69(-6)	21456	1.09(-4)	20087	7.51(-4)	18785	3.02(-3)
2.....	23649	2.85(-5)	22226	3.64(-4)	20864	1.84(-3)	19567	4.46(-3)
	23667	2.95(-5)	22235	3.71(-4)	20867	1.80(-3)	19566	4.46(-3)
3.....	24394	8.27(-5)	22971	8.03(-4)	21610	2.77(-3)	20313	3.68(-3)
	24427	8.55(-5)	22995	8.20(-4)	21627	2.72(-3)	20325	3.69(-3)
4.....	25116	1.78(-4)	23693	1.30(-3)	22331	2.88(-3)	21034	1.58(-3)
	25876	1.83(-4)	23732	1.33(-3)	22363	2.84(-3)	21061	1.59(-3)
5.....	25813	3.04(-4)	24390	1.63(-3)	23029	2.11(-3)	21732	1.63(-4)
	25876	3.09(-4)	24444	1.68(-3)	23074	2.09(-3)	21773	1.61(-4)
6.....	26487	4.29(-4)	25064	1.65(-3)	23703	1.02(-3)	22406	1.35(-4)
	26565	4.28(-4)	25133	1.71(-3)	23764	1.02(-3)	22462	1.41(-4)
7.....	27137	5.13(-4)	25714	1.38(-3)	24353	2.43(-4)	23056	7.52(-4)
	27229	4.96(-4)	25797	1.43(-3)	24428	2.44(-7)	23126	7.79(-4)
8.....	27761	5.3(-4)	26337	9.38(-4)	24976	1.25(-7)	23679	1.08(-3)
	27868	4.88(-4)	26436	9.92(-4)	25067	2.95(-7)	23765	1.13(-3)
9.....	28355	4.70(-4)	26932	5.18(-4)	25571	1.25(-4)	24274	8.67(-4)
	28479	4.07(-4)	27047	5.67(-4)	25678	1.18(-4)	24376	9.49(-4)
10.....	28917	3.66(-4)	27494	2.23(-4)	26133	3.25(-4)	24835	4.36(-4)
	29060	2.83(-4)	27628	2.61(-4)	26259	3.11(-4)	24957	5.14(-4)
11.....	29443	2.47(-4)	28020	6.65(-5)	26659	4.2(-4)	25362	1.15(-4)
	29609	1.58(-4)	28177	9.24(-5)	26808	4.01(-4)	25506	1.64(-4)
12.....	29930	1.44(-4)	28507	9.37(-6)	27146	3.94(-4)	25849	2.68(-6)
	30123	6.21(-5)	28691	2.22(-5)	27322	3.64(-4)	26020	1.48(-5)
13.....	30375	6.94(-5)	28952	8.01(-8)	27591	2.98(-4)	26294	2.60(-5)
	30597	1.13(-5)	29165	2.53(-6)	27796	2.59(-4)	26494	7.73(-6)
14.....	30775	2.56(-5)	29351	4.37(-6)	27990	1.94(-4)	26693	8.47(-5)
	31023	2.66(-7)	29591	8.99(-10)	28222	1.53(-4)	26920	4.45(-5)

Table 3—Continued

	$(X^2\Sigma^+) v'' = 0$		$v'' = 1$		$v'' = 2$		$v'' = 3$	
$v' (B' \ ^2\Sigma^+)$	$E_{v'0}$	$f_{v'0}$	$E_{v'1}$	$f_{v'1}$	$E_{v'2}$	$f_{v'2}$	$E_{v'3}$	$f_{v'3}$

\*Band oscillator strengths are given in a.u. and are calculated for rotational quantum numbers  $N'' = 0$  and  $N' = 1$ . Our results are listed on the first line, with the previous calculations of Kirby et al. (1979) below. Notation:  $x(-n) \equiv x \times 10^{-n}$ .

†Energies  $E_{v'v''}$  of the absorbed photon are given in  $\text{cm}^{-1}$ . Our values are listed on the first line, with the experimental transition energies given by Balfour & Cartwright (1976) below (generally as listed in Kirby et al. 1979), for  $N'' = 0$  and  $N' = 1$ .

Table 4. Line Oscillator Strengths and Transition Energies<sup>a</sup> for the  $B' \ ^2\Sigma^+ \leftarrow X \ ^2\Sigma^+$  System

Band	Line	$f_{v'N',v''N''}^b$	Transition Energy		
			Theory <sup>b</sup>	Observation <sup>c</sup>	$\Delta E$
0-7	P(15)	7.70(-3)	13179.6	13193.61	14.0
	R(19)	7.55(-3)	13175.8	13205.15	29.4
	P(14)	7.85(-3)	13225.2	13237.05	11.9
	R(18)	7.89(-3)	13216.9	13242.93	26.1
	P(13)	7.98(-3)	13268.9	13278.84	10.0
	R(17)	8.18(-3)	13257.3	13280.11	22.8
	R(16)	8.42(-3)	13296.4	13316.39	20.0
	P(12)	8.07(-3)	13310.6	13318.80	8.2
	R(15)	8.62(-3)	13334.1	13351.47	17.4
	P(11)	8.14(-3)	13350.1	13356.71	6.7
	R(14)	8.79(-3)	13370.1	13385.11	15.0
	P(10)	8.19(-3)	13387.2	13392.43	5.2
	R(13)	8.93(-3)	13404.1	13416.97	12.9
	P(9)	8.21(-3)	13421.8	13425.78	4.0
	R(12)	9.06(-3)	13436.1	13446.96	10.9
	P(8)	8.22(-3)	13453.8	13456.70	2.9
	R(11)	9.17(-3)	13465.7	13474.86	9.2
	P(7)	8.19(-3)	13483.0	13485.04	2.1
	R(10)	9.27(-3)	13492.9	13500.49	7.6
	P(6)	8.14(-3)	13509.4	13510.67	1.3
	R(9)	9.36(-3)	13517.6	13523.74	6.2
	P(5)	8.05(-3)	13532.8	13533.51	0.7
	R(8)	9.45(-3)	13539.6	13544.47	4.9
	R(7)	9.54(-3)	13558.8	13562.57	3.8
	R(6)	9.65(-3)	13575.2	13577.93	2.7
	P(2)	7.14(-3)	13585.4	13584.94	0.5
	R(4)	9.98(-3)	13599.1	13600.26	1.2
	R(3)	1.026(-2)	13606.5	13607.03	0.5
	R(2)	1.077(-2)	13610.8	13610.87	0.1

Table 4—Continued

Band	Line	$f_{v'N',v''N''}^b$	Transition Energy		
			Theory <sup>b</sup>	Observation <sup>c</sup>	$\Delta E$
0-6	P(25)	1.093(-2)	13375.2	13394.04	18.9
	P(24)	1.093(-2)	13448.6	13463.80	15.2
	P(20)	1.053(-2)	13734.8	13738.70	3.9
	P(19)	1.037(-2)	13802.9	13804.61	1.7
	R(17)	1.080(-2)	14106.7	14108.39	1.7
	P(13)	9.41(-3)	14164.4	14156.84	7.6
	R(16)	1.063(-2)	14158.9	14158.82	0.1
	P(12)	9.26(-3)	14215.2	14206.61	8.6
	R(15)	1.048(-2)	14208.6	14206.85	1.8
	P(10)	8.97(-3)	14307.6	14297.17	10.5
	P(9)	8.82(-3)	14348.9	14337.75	11.2
	R(10)	9.91(-3)	14413.3	14405.25	8.1
	R(9)	9.83(-3)	14444.7	14435.66	9.1
	P(6)	8.37(-3)	14452.2	14439.50	12.7
	P(2)	7.10(-3)	14539.8	14526.15	13.7
	1-8	P(14)	1.055(-2)	13295.8	13346.85
P(13)		1.074(-2)	13324.4	13372.71	48.3
P(12)		1.085(-2)	13352.6	13398.60	46.0
P(11)		1.088(-2)	13380.1	13423.95	43.9
P(10)		1.085(-2)	13406.4	13448.42	42.0
P(9)		1.077(-2)	13431.5	13471.80	40.3
P(8)		1.067(-2)	13455.1	13493.88	38.8
R(14)		1.171(-2)	13440.9	13494.45	53.6
P(7)		1.053(-2)	13477.1	13514.50	37.4
R(12)		1.204(-2)	13478.3	13527.31	49.0
R(11)		1.210(-2)	13495.9	13542.34	46.5
P(5)		1.015(-2)	13515.4	13550.76	35.4
R(9)		1.212(-2)	13527.7	13569.96	42.3
R(8)		1.212(-2)	13541.3	13581.87	40.6

Table 4—Continued

Band	Line	$f_{v'N',v''N''}^b$	Transition Energy		
			Theory <sup>b</sup>	Observation <sup>c</sup>	$\Delta E$
	R(7)	1.213(-2)	13553.2	13592.23	39.1
	R(5)	1.223(-2)	13571.3	13607.90	36.6
0-5	P(25)	8.96(-3)	14240.0	14237.01	3.0
	R(28)	1.065(-2)	14229.6	14239.89	10.3
	P(23)	8.20(-3)	14421.3	14414.50	6.8
	P(21)	7.53(-3)	14594.6	14584.70	9.9
	P(20)	7.24(-3)	14677.7	14666.55	11.2
	R(22)	8.07(-3)	14728.8	14725.08	3.7
	P(19)	6.97(-3)	14758.2	14745.82	12.4
	P(18)	6.73(-3)	14835.9	14822.42	13.5
	P(17)	6.50(-3)	14910.7	14896.23	14.5
	R(19)	7.20(-3)	14950.5	14942.21	8.3
	P(16)	6.28(-3)	14982.3	14967.00	15.3
	R(18)	6.96(-3)	15018.8	15009.35	9.5
	P(15)	6.09(-3)	15050.7	15034.68	16.0
	R(17)	6.74(-3)	15084.2	15073.52	10.7
	P(14)	5.91(-3)	15115.8	15099.05	16.8
	R(16)	6.55(-3)	15146.4	15134.66	11.8
	P(13)	5.74(-3)	15177.3	15160.02	17.3
	R(15)	6.37(-3)	15205.2	15192.54	12.7
	P(12)	5.59(-3)	15235.3	15217.47	17.9
	R(14)	6.21(-3)	15260.7	15247.07	13.7
	R(13)	6.07(-3)	15312.6	15298.15	14.5
	P(10)	5.32(-3)	15340.2	15321.39	18.6
	R(11)	5.84(-3)	15405.3	15389.47	15.9
	P(8)	5.07(-3)	15429.6	15410.12	19.5
	R(10)	5.75(-3)	15445.9	15429.45	16.5
	P(7)	4.95(-3)	15468.3	15448.59	19.7
	R(9)	5.68(-3)	15482.7	15465.61	17.1

Table 4—Continued

Band	Line	$f_{v'N',v''N''}^b$	Transition Energy		
			Theory <sup>b</sup>	Observation <sup>c</sup>	$\Delta E$
	P(6)	4.84(-3)	15502.9	15483.00	19.9
	R(8)	5.63(-3)	15515.5	15497.85	17.7
	R(5)	5.60(-3)	15589.2	15570.34	18.9
	R(4)	5.65(-3)	15605.5	15586.26	19.3
1-7	P(12)	4.51(-3)	14103.7	14124.76	21.1
	P(11)	4.16(-3)	14143.0	14162.53	19.6
	R(14)	5.35(-3)	14163.6	14191.01	27.4
	P(10)	3.85(-3)	14180.0	14198.15	18.2
	R(11)	4.24(-3)	14258.9	14280.92	22.0
0-4	R(30)	5.33(-3)	14959.6	14957.45	2.2
	R(29)	4.94(-3)	15066.5	15062.38	4.1
	P(26)	4.09(-3)	15121.8	15107.35	14.5
	R(28)	4.59(-3)	15171.9	15165.97	6.0
	P(25)	3.83(-3)	15229.6	15213.99	15.6
	R(27)	4.28(-3)	15275.4	15267.86	7.6
	P(24)	3.61(-3)	15334.9	15318.38	16.5
	R(25)	3.76(-3)	15475.9	15465.61	10.3
	P(22)	3.22(-3)	15537.6	15519.37	18.3
	R(24)	3.55(-3)	15572.5	15561.01	11.5
	P(21)	3.06(-3)	15634.6	15615.65	19.0
	P(20)	2.91(-3)	15728.4	15708.90	19.5
	R(22)	3.18(-3)	15757.3	15743.80	13.5
	R(21)	3.03(-3)	15845.2	15830.84	14.4
	P(18)	2.65(-3)	15906.1	15885.62	20.5
	P(13)	2.20(-3)	16286.1	16264.10	22.0
	R(15)	2.40(-3)	16300.2	16282.03	18.2
	R(14)	2.33(-3)	16362.8	16344.15	18.7
	P(11)	2.07(-3)	16410.0	16387.72	22.3
	R(13)	2.27(-3)	16421.3	16402.22	19.1

Table 4—Continued

Band	Line	$f_{v'N',v''N''}^b$	Transition Energy		
			Theory <sup>b</sup>	Observation <sup>c</sup>	$\Delta E$
	P(10)	2.01(-3)	16465.6	16443.22	22.4
	R(12)	2.22(-3)	16475.6	16456.16	19.5
	P(9)	1.96(-3)	16516.9	16494.39	22.5
	R(11)	2.18(-3)	16525.7	16505.78	19.9
	P(8)	1.91(-3)	16563.7	16541.06	22.7
	R(10)	2.14(-3)	16571.4	16551.19	20.2
1-4	R(25)	4.35(-3)	16268.3	16269.70	1.4
	P(22)	3.96(-3)	16331.2	16325.20	6.0
	R(24)	4.29(-3)	16365.2	16366.09	0.9
	R(23)	4.23(-3)	16459.4	16458.93	0.5
	P(20)	3.85(-3)	16522.1	16514.96	7.2
	R(22)	4.17(-3)	16550.6	16549.22	1.4
	P(19)	3.79(-3)	16612.7	16605.04	7.7
	R(21)	4.11(-3)	16638.7	16636.50	2.2
	P(18)	3.74(-3)	16699.8	16691.68	8.1
	R(20)	4.05(-3)	16723.5	16720.58	2.9
	P(17)	3.68(-3)	16783.3	16774.87	8.5
	R(19)	3.99(-3)	16804.9	16801.32	3.6
	P(16)	3.63(-3)	16863.1	16854.32	8.8
	R(18)	3.94(-3)	16882.8	16878.57	4.3
	P(14)	3.53(-3)	17011.2	17002.58	8.7
	P(13)	3.47(-3)	17079.3	17070.15	9.2
	P(12)	3.43(-3)	17143.3	17133.95	9.4
	R(14)	3.76(-3)	17156.3	17150.10	6.2
	P(11)	3.38(-3)	17203.0	17193.56	9.5
	P(10)	3.33(-3)	17258.5	17248.93	9.6
	P(9)	3.29(-3)	17309.6	17299.97	9.7
	R(11)	3.67(-3)	17318.9	17311.93	7.0
	P(8)	3.24(-3)	17356.3	17346.63	9.7

Table 4—Continued

Band	Line	$f_{v'N',v''N''}^b$	Transition Energy		
			Theory <sup>b</sup>	Observation <sup>c</sup>	$\Delta E$
	R(10)	3.64(-3)	17364.5	17357.26	7.3
	P(7)	3.19(-3)	17398.5	17388.84	9.7
	R(9)	3.63(-3)	17405.7	17398.15	7.6
	P(6)	3.13(-3)	17436.2	17426.59	9.6
	R(6)	3.64(-3)	17502.3	17494.03	8.3
	R(5)	3.67(-3)	17525.3	17516.87	8.5
1-3	P(31)	3.13(-3)	16348.2	16341.26	7.0
	P(30)	2.99(-3)	16481.4	16473.62	7.8
	R(32)	3.23(-3)	16515.9	16517.06	1.2
	P(29)	2.86(-3)	16612.4	16603.90	8.5
	R(31)	3.08(-3)	16643.3	16642.44	0.9
	P(28)	2.73(-3)	16741.0	16731.92	9.1
	R(30)	2.93(-3)	16768.5	16766.68	1.8
	P(27)	2.62(-3)	16867.0	16857.35	9.7
	R(29)	2.80(-3)	16891.5	16888.77	2.8
	P(25)	2.42(-3)	17110.5	17100.35	10.2
	P(24)	2.33(-3)	17227.6	17217.19	10.4
	R(26)	2.47(-3)	17244.4	17239.72	4.7
	P(23)	2.24(-3)	17341.5	17330.87	10.7
	P(22)	2.16(-3)	17451.9	17441.15	10.8
	R(24)	2.29(-3)	17464.6	17459.51	5.1
	P(21)	2.09(-3)	17558.7	17547.92	10.8
	R(23)	2.21(-3)	17569.7	17563.93	5.8
	P(20)	2.03(-3)	17661.8	17651.02	10.8
	P(19)	1.96(-3)	17761.1	17750.31	10.8
	R(21)	2.07(-3)	17769.2	17762.78	6.5
	P(18)	1.91(-3)	17856.4	17845.65	10.8
	P(17)	1.85(-3)	17947.6	17936.95	10.7
	R(19)	1.96(-3)	17953.3	17946.66	6.7

Table 4—Continued

Band	Line	$f_{v'N',v''N''}^b$	Transition Energy		
			Theory <sup>b</sup>	Observation <sup>c</sup>	$\Delta E$
	R(17)	1.87(-3)	18121.3	18114.28	7.0
	P(12)	1.64(-3)	18339.0	18329.33	9.7
	P(10)	1.58(-3)	18463.7	18454.34	9.4
	P(9)	1.54(-3)	18518.9	18509.52	9.4
	R(11)	1.69(-3)	18519.6	18512.55	7.1
	P(7)	1.48(-3)	18614.8	18605.96	8.9
0-3	P(22)	8.4(-4)	16658.3	16635.32	23.0
	R(23)	8.5(-4)	16776.7	16758.79	17.9
	R(20)	7.2(-4)	17069.6	17050.78	18.9
	P(17)	6.5(-4)	17154.0	17130.89	23.1
	P(16)	6.3(-4)	17241.1	17218.08	23.0
	R(17)	6.4(-4)	17327.5	17308.15	19.4
	R(15)	6.0(-4)	17478.5	17458.90	19.6
	P(12)	5.4(-4)	17545.9	17523.37	22.6
	R(12)	5.5(-4)	17671.4	17651.53	19.9

<sup>a</sup>In  $\text{cm}^{-1}$ .

<sup>b</sup>This work.

<sup>c</sup>Wallace et al. (1999).